Mercury-Based Cuprate High–Transition Temperature Grain-Boundary Junctions and SQUIDs Operating Above 110 Kelvin

A. Gupta, J. Z. Sun, C. C. Tsuei

The superconducting transport characteristics of $HgBa_2CaCu_2O_{6+\delta}$ (Hg-1212) films and grain-boundary junctions grown on (100)-oriented $SrTiO_3$ bicrystal substrates have been investigated. The films exhibit a zero-resistance temperature of ~120 kelvin and sustain large critical current densities, with values as high as 10^6 amperes per square centimeter at around 100 kelvin. On the other hand, the grain boundaries behave as weak links, with substantially lower critical currents, as is observed for other cuprate superconductors. A reduction of three orders of magnitude in critical current was observed for transport across a 36.8° grain boundary. The current-voltage characteristics of bridges across such a grain boundary show weak-link behavior qualitatively resembling that of a resistively shunted junction. Single-level direct-current superconducting quantum interference devices (SQUIDs) have been fabricated with such bicrystal junctions. These SQUIDs show clear periodic voltage modulations when subjected to applied magnetic fields. The SQUIDs operate at temperatures as high as 111.8 kelvin, which makes them attractive for operation in portable sensors and devices that utilize nonconventional cooling methods.

Grain boundaries (GBs) of high–transition temperature (T_c) cuprates have been extensively studied in recent years. High-angle GBs in these materials are known to form superconducting weak links. In particular, with the use of bicrystal grain-boundary junctions (GBJs) of $YBa_2Cu_3O_{7-\delta}$ (YBCO) and also other cuprates, it has been shown that for small misorientation angles the GB critical current is determined by flux flow and by Josephson junction–like coupling for larger angles ($\theta \geq 15°$) (*1–3*). The weak-link characteristics of high-angle GBJs has been gainfully exploited for the controllable and reproducible fabrication of relatively low-noise dc SQUIDs operating at liquid nitrogen temperature (77 K) (*4, 5*).

Although operation at 77 K is considered adequate for a number of applications involving SQUIDs and also microwave devices, higher temperature operation is desirable in cases where liquid nitrogen cooling is difficult or inconvenient to implement. These include spaceborne applications involving passively cooled devices and also portable sensors and communication equipment that make use of miniature cryocoolers with low power consumption (*6*). For operation above liquid nitrogen temperatures, particularly above 100 K, it is necessary to investigate the device characteristics of superconducting cuprates of higher T_c's than YBCO. In addition to providing higher operating temperatures, the higher T_c materials can also improve the performance of the devices when they are operated at 77 K.

The highest T_c's in the cuprate family (>120 K) have so far been observed in the Hg- and Tl-based materials. For the mercury cuprates, $HgBa_2Ca_{n-1}Cu_nO_{2n+2+\delta}$, the bulk Hg-1212 ($n = 2$) and Hg-1223 ($n = 3$) phases have T_c's of 125 and 135 K, respectively (*7*). Although the T_c of the bulk Tl-2223 system can also be as high as 125 K, the more readily available T1-2212 phase has a zero-resistance temperature of about 110 K. Thin films of Tl-2212, which generally exhibit T_c's of 100 to 105 K, are presently considered the most practical for device applications at operating temperatures higher than those possible with YBCO.

Recently we reported on the synthesis of high-quality films of $HgBa_2CaCu_2O_{6+\delta}$ (Hg-1212) with a zero-resistance T_c as high as 124 K (*8*). We report here the fabrication of GBJ devices with our Hg-1212 film process, using 36.8° $SrTiO_3$ bicrystals as substrates. Clear weak-link behavior was obtained in such GBJ devices at temperatures well above 100 K. We have also fabricated dc SQUIDs using these junctions. Large SQUID voltage modulation was observed as a function of the applied magnetic field. This SQUID signal was clearly observable with sample temperatures as high as 111.8 K.

The growth of Hg-1212 films from precursor oxides has been described (*8*). Briefly, the pulsed laser deposition technique is used to deposit sequential layers of HgO and the cuprate precursor $Ba_2CaCu_2O_x$ from two separate targets. To ensure that the desired stoichiometric composition is achieved, we have made routine use of Rutherford backscattering measurements for calibrating the amount of material deposited per pulse from the individual targets. The films are deposited at room temperature in a vacuum atmosphere on (100)-oriented $SrTiO_3$ substrates. To achieve good thickness uniformity, the substrates are placed on a holder that is slowly rotated during the deposition process. For this work, the total film thickness is of the order of 0.25 to 0.30 μm, which is significantly thinner than what we used in our previous study (*8*). A layer of HgO 400 Å thick is deposited as a final protective cover layer.

The as-deposited films are amorphous and must be annealed at high temperatures to form the superconducting phase. The films are annealed at 800°C for 1 hour in sealed quartz ampules together with appropriate amounts of bulk stoichiometric mercury cuprate and pellets of the precursor. The proper combination of bulk materials is chosen to provide the appropriate Hg atmosphere and O_2 partial pressure that are consistent with the thermodynamic requirements for stabilizing the Hg-1212 phase at the annealing temperature. The details are provided elsewhere (*8*).

For the GBJ and SQUID measurements, films have been deposited on commercially available bicrystal $SrTiO_3$ substrates and subsequently annealed. The bicrystals we used contain symmetric (001) tilt boundaries with a misorientation angle of 36.8°. The films are patterned by means of laser ablation to form junctions or lines, with feature sizes of 10 μm or larger. Critical currents have been measured both in the film and across the grain boundary. These patterned films are quite robust and can withstand repeated thermal cycling from room temperature to 77 K, with exposure to the atmosphere for short periods between the cycles without any observable changes in the transport properties. Moreover, the films can be stored indefinitely in a nitrogen atmosphere with minimal degradation.

X-ray diffraction analyses have shown that the films are essentially phase-pure Hg-1212, with the *c* axis (12.54 Å) aligned normal to the plane of the substrate. Weak diffraction peaks corresponding to small amounts of impurity phases are also observed (*8*). Most of these peaks can be indexed to the single-layer Hg-1201 phase. Optical inspection of the films reveals that most of the secondary phases are present as precipitates, which are randomly distributed in an otherwise smooth film matrix. These precipitates are of dimension ~0.5 to 1.0 μm and are the primary source of film roughness.

Despite the presence of some secondary phases, the Hg-1212 films exhibit excellent transport properties. They display a metallic behavior, with positive temperature intercept, in the normal state and a sharp superconducting transition. Zero-resistance temperatures of 120 to 122 K are routinely observed for these films. A typical resistance plot for a Hg-1212 film 0.25 μm thick is shown in Fig. 1 (inset).

IBM Research Division, Thomas J. Watson Research Center, Yorktown Heights, NY 10598, USA.

The high electrical quality of the films is also evidenced by the fact that they can sustain relatively high critical currents, even at temperatures above 100 K. Figure 1 shows the temperature dependence of the zero-field critical current density (J_c) of the film on the basis of a threshold criterion of 1 μV/mm. A J_c of $\sim 10^6$ A/cm^2 is observed at 100 K, which is at least an order of magnitude higher than those observed in Tl-based films (*3*, *9*). Unfortunately, the transport critical current could not be measured at much lower temperatures because of poor contacts, which result in excessive heating and catastrophic failure at high currents (>100 mA). However, using the Bean model (*10*), we have made magnetic measurements to estimate the critical currents at lower temperatures. We estimate J_c values of 2×10^7 A/cm^2 at 10 K and $\sim 4 \times 10^6$ A/cm^2 at 77 K. These values are similar to those observed for high-quality YBCO films at these temperatures.

The GB current-voltage (*I-V*) characteristics and J_c as a function of temperature for a film deposited on a bicrystal substrate, with a misorientation angle of 36.8°, are plotted in Fig. 2. The GB behaves as a weak link with *I-V* curves similar to those expected according to the resistively shunted junction model. The GB supercurrent (I_c) decreases with increasing temperature and persists up to 114 K (Fig. 2). At a temperature of 100 K, the GB J_c is about three orders of magnitude lower than that observed for the film. The I_cR_n product of the junction we have measured, where R_n is the asymptotic resistance, falls in the range of 60 to 120 μV at 77 K. The values for J_c and the I_cR_n product for the 36.8° Hg-1212 GBJ are quite similar to those observed for YBCO films (*2*). Moreover, the temperature dependence of J_c is also qualitatively in accord with the behavior observed for GBJs of YBCO and other high-T_c cuprates.

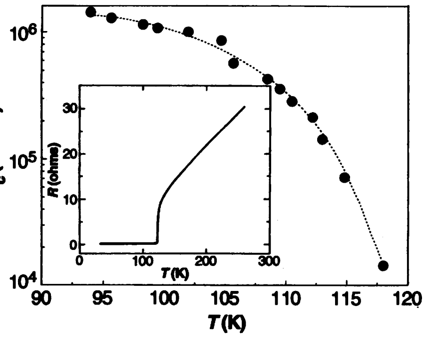

Fig. 1. Temperature dependence of the critical current density for a 0.25-μm-thick Hg-1212 film. The data have been obtained from transport measurements of 20-μm microbridges formed by laser patterning. A voltage criterion of 1 μV/mm was used for the measurements. (**Inset**) A typical resistive transition for such films after laser patterning.

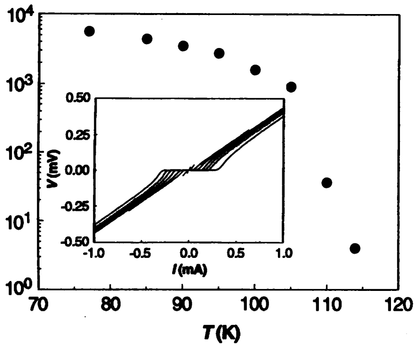

Fig. 2. Temperature dependence of the critical current density for a 10-μm-wide microbridge across a 36.8° grain boundary. (**Inset**) The *I-V* characteristics at different temperatures (from high I_c to low I_c: 77, 85, 90, 95, 100, 105, 110, and 114 K).

With laser patterning, such GBJs were used to form simple SQUID structures across bicrystal grain boundaries. The dc SQUIDs consist of pairs of 10- or 20-μm-wide junctions with square-shaped SQUID loop holes that are 10 to 20 μm on each side. A schematic drawing of the SQUID structure, along with the observed voltage modulation as a function of the perpendicular magnetic field at 77 K, is shown in Fig. 3. The modulation period corresponds to one flux quantum (Φ_0) in the SQUID loop. The SQUID consists of junctions 10 μm wide with an estimated loop inductance around 30 pH (pH = picohenry). Because the width of the GBJ and the dimensions of the SQUID are comparable in this structure, the SQUID modulation is superimposed on the central lobe of the longer wavelength modulation resulting from the flux threading the area of the junctions. Regardless, periodic voltage modulation is observed over a relatively wide range of applied field. For sweeping fields with peak-to-peak amplitude above 400 mG, an onset of magnetic hysteresis was observed in the SQUID response. This is presumably caused by flux entry or movement of pinned vortices in the film.

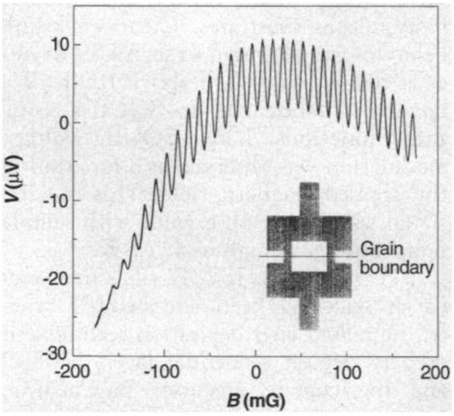

Fig. 3. SQUID modulation as a function of the applied field at 77 K. A sketch of the device structure is shown in the inset. The weak links are 10 μm wide, and the center hole is 20 μm on each side. No visible hysteresis in SQUID response was observed for sweeping fields of amplitude below 400 mG peak to peak.

These SQUIDs were observed to operate at record high temperatures. The temperature dependence of the optimal $V(\Phi)$ peak-to-peak voltage is plotted in Fig. 4, with the insets showing the actual $V(\Phi)$ transfer function at 77 and 107 K, respectively. The peak-to-peak voltage of about 9.5 μV at 77 K compares well with that observed for YBCO bicrystal SQUIDs. As expected, at higher temperatures the amplitude of the voltage modulation decreases because of the drop in I_cR_n. Nevertheless, even at temperatures above 100 K the response is surprisingly good, with a modulation amplitude of about 2.5 μV at 107 K, corresponding to a flux responsivity $dV/d\Phi$ of ~ 8 μV/Φ_0. The relatively noisy field response at 107 K (Fig. 4) is largely instrument-limited because of insufficient averaging (average of two to three traces). On the other hand, the response at 77 K, because of temperature stability, has been averaged over 20 traces. The highest temperature at which we were able to obtain a measurable signal from the SQUID is 111.8 K. It is expected that even higher temperature operation is feasible with optimization of the SQUID parameters.

The noise characteristics of these junction devices are being investigated. Our preliminary results with the Hg-1212 SQUID show that, at 77 K, the predominant low-frequency noise has a $1/f$ spectrum, as is also common in YBCO and Tl-2212-based SQUIDs. A flux noise power, S_Φ, of $\sim 10^{-6}$ Φ_0^2/Hz at 1 Hz was measured with a flux-locked loop on one of our SQUIDs. This noise figure is about an order

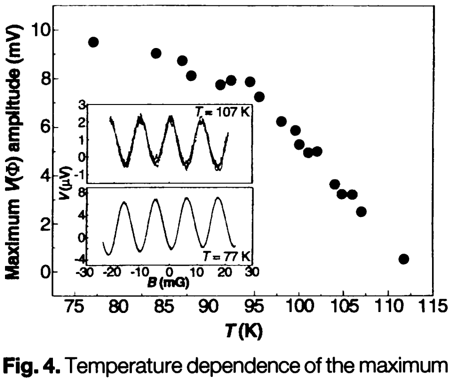

Fig. 4. Temperature dependence of the maximum SQUID transfer function. The SQUID has the same geometry as described in Fig. 3. The critical current for this SQUID is 280 μA at 77 K. (**Inset**) The $V(\Phi)$ transfer functions at 77 and 107 K. The difference in apparent noise in these two plots is largely a result of a difference in the number of traces that were averaged.

of magnitude higher than that measured in a typical YBCO SQUID with similar parameters.

The feasibility demonstration of Hg-based cuprate SQUIDs operating above 110 K appears promising and expands the possibility of utilizing integrated microcooling techniques, such as Joule-Thompson or on-chip thermoelectric refrigeration, for superconducting electronic applications. Joule-Thompson microcoolers that operate at temperatures down to 77 K are commercially available. On the other hand, more development work is necessary to allow operation of cryogenic thermoelectric coolers at temperatures below 150 K. The design of composite systems consisting of a battery of thermoelectric coolers for operation at lower temperatures has recently been proposed (*11*).

REFERENCES AND NOTES

1. P. Chaudhari *et al.*, *Phys. Rev. Lett.* **60**, 1653 (1988).
2. B. H. Moeckly, D. K. Lathrop, R. A. Buhrman, *Phys. Rev. B* **47**, 400 (1993); R. Gross, P. Chaudhari, M. Kawasaki, A. Gupta, *ibid.* **42**, 10735 (1990).
3. A. H. Cardona, H. Suzuki, T. Yamashita, K. H. Young, L. C. Bourne, *Appl. Phys. Lett.* **62**, 411 (1993); M. Kawasaki *et al.*, *ibid.*, p. 417.
4. A. H. Miklich *et al.*, *IEEE Trans. Appl. Supercond.* **3**, 2434 (1993); R. Gross, P. Chaudhari, M. Kawasaki, M. B. Ketchen, A. Gupta, *Appl. Phys. Lett.* **57**, 727 (1990).
5. K. Char, M. S. Colclough, L. P. Lee, G. Zaharchuk, *Appl. Phys. Lett.* **59**, 2177 (1991).
6. For example, see G. Walker, *Miniature Refrigerators for Cryogenic Sensors and Cold Electronics* (Oxford, Univ. Press, London, 1989).
7. A. Schilling, M. Cantori, J. D. Guo, H. R. Ott, *Nature* **363**, 56 (1993).
8. C. C. Tsuei, A. Gupta, G. Trafas, D. Mitzi, *Science* **263**, 1259 (1994).
9. W. Y. Lee *et al.*, *Appl. Phys. Lett.* **60**, 772 (1992).
10. C. P. Bean, *Phys. Rev. Lett.* **8**, 250 (1962).
11. V. A. Kutasov *et al.*, *Sov. Tech. Phys. Lett.* **18**, 542 (1992); Z. M. Dashevskii *et al.*, *Supercond. Sci. Technol.* **5**, 690 (1992).

12. We thank G. Trafas for technical assistance and L. S. Yu-Jahnes, W. J. Gallagher, and M. B. Ketchen for helpful discussions.

16 May 1994; accepted 27 June 1994

Single-Crystalline $(KC_{60})_n$: A Conducting Linear Alkali Fulleride Polymer

S. Pekker,* A. Jánossy, L. Mihaly, O. Chauvet,
M. Carrard, L. Forró

Single crystals of a linear cycloadduct conducting polymer, $(KC_{60})_n$, have been grown that are a few tenths of a millimeter in length. Partial oxidation under toluene transformed these crystals into bundles of fibers. The degree of polymerization exceeded 100,000.

The large-scale production (*1*) of C_{60} has initiated an intensive research effort for the isolation of higher fullerenes (*2*) and the synthesis of fullerene derivatives with interesting physical and chemical properties (*3*). Rao *et al.* (*4*) reported a photoinduced polymerization of C_{60} films and hypothesized that it resulted from the formation of a [2 + 2] cycloadduct linkage. The synthesis of conducting alkali fullerides (*5*) also opened a new field of research. Recently, the unusual physical properties of A_1C_{60} (A=K, Rb, and Cs) compounds came into focus. A rather unusual phase transition has been observed at about 400 K in optical (*6*) and electron spin resonance (*7*) (ESR) spectra and in differential scanning calorimetry (*8*). The initial suggestion of Winter and Kuzmany (*6*) that the high-temperature phase has a face-centered cubic (fcc) "rock salt" structure with C_{60} ions surrounded by eight alkali metal ions was confirmed by the x-ray diffraction (XRD) studies of Zhu *et al.* (*8*). Chauvet *et al.* (*9*) showed that the low-temperature structure of Rb_1C_{60} is orthorhombic (o-Rb_1C_{60}) with an unusually short separation of 9.1 Å between the centers of C_{60} molecules along the crystallographic **a** direction. An isostructural phase of K_1C_{60} was observed at ambient temperature in XRD studies (*10*).

Pekker *et al.* (*11*) suggested that the anions in the orthorhombic phase of A_1C_{60} compounds are linear polymers formed by an ionically induced reversible [2 + 2] cycloaddition reaction of the fulleride ions in the solid state at about 400 K. It was argued that the forbidden [2 + 2] cycloaddition of ground-state neutral molecules is thermally allowed between the singly charged fulleride anions. The proposed structure of the cycloadduct polyanion (Fig. 1) is supported by a Rietveld refinement (*12*) of powder XRD data. In this report, we provide further evidence for the polyanions. We have grown large single crystals of orthorhombic K_1C_{60} that are unexpectedly stable in air. Long fibers of orthorhombic K_1C_{60} apparent in crystals that were treated with organic solvents in air are evidence for a high degree of polymerization.

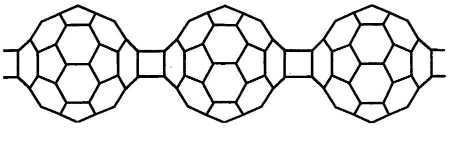

Fig. 1. Molecular view of the [2 + 2] cycloadduct $(C_{60})_n$ polyanion.

The K_1C_{60} single crystals were prepared by a new coevaporation method. Stoichiometric amounts of C_{60} and K were sealed in a quartz tube that was heated in a gradient furnace. The temperatures of C_{60} and K were 600° and 150°C, respectively. A microcrystalline film of K_1C_{60} coated the wall of the tube at about the 300°C zone within a few hours, and single crystals embedded in a microcrystalline matrix grew in 3 days. A typical region with a few single crystals is shown in the optical micrograph in Fig. 2. The typical dimensions of the largest crystals are 200 μm by 100 μm by 100 μm. Only microcrystalline alkali metal salts of C_{60} have been prepared by coevaporation previously (*13*).

In Fig. 3 we compare the temperature dependence of the ESR linewidths of a few large coevaporated single crystals to that of a K_1C_{60} powder composed of a few crystallites in the micrometer size range. The powder was prepared in a usual way (*5*) by solid-state reaction of a stoichiometric mixture of C_{60} and K in a sealed quartz capillary at 260°C for 80 days. The ESR spectrum of the coevaporated single crystals shows that they are indeed o-K_1C_{60}. The ESR linewidths of the single crystals and the powder K_1C_{60} sample are nearly the same, and both show a hysteretic transition in the temperature range of the polymerization. The magnetic spin susceptibility decreases by a factor of 2 during the polymerization. A similar narrowing of the linewidth and a small decrease of susceptibility with decreasing temperature was observed (*7*, *9*) upon polymerization of Rb_1C_{60}. Although we have no XRD evidence, the magnetic characteristics and the phase transition above 350 K make it very likely that the single crystals are composed of K_1C_{60}.

We have studied the stability of the crystals against oxygen and solvents. We exposed a few coevaporated single crystals to air and monitored the variation of the ESR signal at room temperature. The intensity of the signal was constant over a few

---

S. Pekker, Research Institute for Solid State Physics, H-1525 Budapest, P. O. B. 49, Hungary, and Laboratoire de Physique des Solides Semicrystallins, IGA Department de Physique, Ecole Polytechnique Federale de Lausanne, 1015-Lausanne, Switzerland.
A. Jánossy, Research Institute for Solid State Physics, H-1525 Budapest, P. O. B. 49, Hungary, and Institute of Physics of the Technical University, H-1521 Budapest, Hungary.
L. Mihaly, Department of Physics, State University of New York at Stony Brook, NY 11794-3800, USA.
O. Chauvet, M. Carrard, L. Forró, Laboratoire de Physique des Solides Semicrystallins, IGA Departement de Physique, Ecole Polytechnique Federale de Lausanne, 1015-Lausanne, Switzerland.

*To whom correspondence should be addressed.